Rapid contextualization of fragmented scene information in the human visual system

Daniel Kaiser[1], Gabriele Inciuraite[2], Radoslaw M. Cichy[2,3,4]

[1]*Department of Psychology, University of York, York, UK*

[2]*Department of Education and Psychology, Freie Universität Berlin, Berlin, Germany*

[3]*Berlin School of Mind and Brain, Humboldt-Universität Berlin, Berlin, Germany*

[4]*Bernstein Center for Computational Neuroscience Berlin, Berlin, Germany*

Correspondence:

Dr Daniel Kaiser

Department of Psychology

University of York

Heslington, York

YO10 5DD, UK

danielkaiser.net@gmail.com

21

22 **Abstract**

23

24 Real-world environments are extremely rich in visual information. At any given
25 moment in time, only a fraction of this information is available to the eyes and the
26 brain, rendering naturalistic vision a collection of incomplete snapshots. Previous
27 research suggests that in order to successfully contextualize this fragmented
28 information, the visual system sorts inputs according to spatial schemata, that is
29 knowledge about the typical composition of the visual world. Here, we used a large
30 set of different natural scene fragments to investigate whether this sorting mechanism
31 can operate across the diverse visual environments encountered during real-world
32 vision. We recorded brain activity using electroencephalography (EEG) while
33 participants viewed incomplete scene fragments at fixation. Using representational
34 similarity analysis on the EEG data, we tracked the fragments' cortical
35 representations across time. We found that the fragments' typical vertical location
36 within the environment (top or bottom) predicted their cortical representations,
37 indexing a sorting of information according to spatial schemata. The fragments'
38 cortical representations were most strongly organized by their vertical location at
39 around 200ms after image onset, suggesting rapid perceptual sorting of information
40 according to spatial schemata. Our results identify a cortical sorting process that
41 allows the visual system to efficiently contextualize fragmented inputs. By
42 demonstrating this sorting across a wide range of visually diverse scenes, our study
43 suggests a contextualization mechanism suitable for complex and variable real-world
44 environments.

Keywords: visual perception, scene representation, spatial schema, EEG, representational similarity analysis

Rapid contextualization of fragmented scene information in the human visual system

The visual world around us is structured in predictable ways at multiple levels (Kaiser et al., 2019a). Natural scenes are characterized by typical distributions of low- and mid-level visual features (Geisler, 2008; Oliva & Torralba, 2003; Purves et al., 2011), as well as typical arrangements of high-level contents across the scene (Bar, 2004; Kaiser et al., 2019a; Torralba et al., 2006; Oliva & Torralba, 2007; Vo et al., 2019; Wolfe et al., 2011). The visual system has adapted to this structure: when multiple scene elements are arranged in a typical way, cortical processing is more efficient (Abassi & Papeo, 2019; Baldassano et al., 2016; Bilalic et al., 2019; Gronau et al., 2008; Kim & Biederman, 2011; Kim et al., 2011; Kaiser et al., 2014, 2019b; Kaiser & Peelen, 2018; Roberts & Humphreys, 2010). Such results suggest that when multiple scene elements need to be processed concurrently, cortical processing is strongly tuned to the typical composition of these elements.

In real-life situations, however, we usually do not have access to detailed visual information about all scene elements at once. Instead, visual inputs are fragmented, and only incomplete snapshots of the world are available for visual analysis at any given moment in time. How does the brain assemble a coherent image of the world from such fragmented inputs? To solve this problem, the visual system may draw from internal representations of typical scene structure – scene schemata (Mandler, 1984; Minsky, 1975, Rumelhart, 1980) – in order to contextualize the fragmented inputs with which it is faced. More specifically, schemata may be used to match

fragmented visual inputs with their place in the schema: as a result, fragmented visual information should be sorted according to its typical location within the environment. This sorting may help to efficiently contextualize visual inputs.

A recent study showed that incomplete inputs – fragments of natural scenes – are indeed sorted according to their typical location in real-world environments (Kaiser et al., 2019c): In the occipital place area and after 200ms of vision, representations of scene fragments were organized by their typical vertical location in the world. For instance, fragments that typically appear in the upper part of a scene (e.g., a house roof or the ceiling of a room) were represented more similarly to each other than to fragments that typically appear in the lower part of a scene (e.g., a lawn or the room's floor). No such organization was found for the fragments' horizontal location, for which clear schemata are missing (Mandler & Parker, 1976).

As a critical limitation, our previous study (Kaiser et al., 2019c) only comprised six different scenes. However, for this mechanism to be useful in the real world, it has to operate across huge amounts of vastly different scenes encountered in our everyday lives. We therefore set out to replicate our findings across a larger and more diverse set of scene images. Here, we used a set of 210 indoor and outdoor scenes, which we split into 4 position-specific fragments each, yielding 840 unique scene fragments (Figure 1a). During an EEG experiment, participants viewed each fragment centrally and in isolation (Figure 1b). Using representational similarity analysis (RSA; Kriegeskorte et al., 2018), we then tracked the fragments' cortical representations across time. As the key result, we found that most prominently after 200ms of visual processing, the fragments' cortical representations were organized by their vertical location within the full scene. We conclude that the visual system uses scene

97 schemata to sort inputs according to their typical location within the environment,

98 supporting the contextualization of fragmented visual information.

99

100 ## Materials and Methods

101

102 ### Participants

103 Twenty healthy adults (mean age 27.3, *SD* = 4.6; 12 female) participated in the
104 study. The sample size was identical to the sample size of our previous EEG study
105 (Kaiser et al., 2019c). All participants had normal or corrected-to-normal vision.
106 Participants provided informed consent and received monetary reimbursement or
107 course credits. All procedures were approved by the ethical committee of Freie
108 Universität Berlin and were in accordance with the Declaration of Helsinki.

109

110 ### Stimuli

111 Stimuli were 210 natural scene photographs, taken from an online resource
112 (Konkle et al., 2010). Half of the stimuli depicted outdoor scenes (bridges, camping
113 sites, historical buildings, houses, natural environments, streets, and waterfronts) and
114 half of the stimuli depicted indoor scenes (bathrooms, bedrooms, churches,
115 classrooms, dining rooms, kitchens, and living rooms). To create position-specific
116 fragments, each scene was split along the vertical and horizontal axes (Figure 1a),
117 yielding four fragments of equal size for each scene and 840 fragments in total. The
118 full stimulus set is available on OSF (doi.org/10.17605/OSF.IO/D7P8G). During the
119 experiment, these fragments were presented individually and in the center of the
120 screen (5.5° by 5.5° visual angle). Participants were not shown the full scene images
121 prior to the experiment.

122

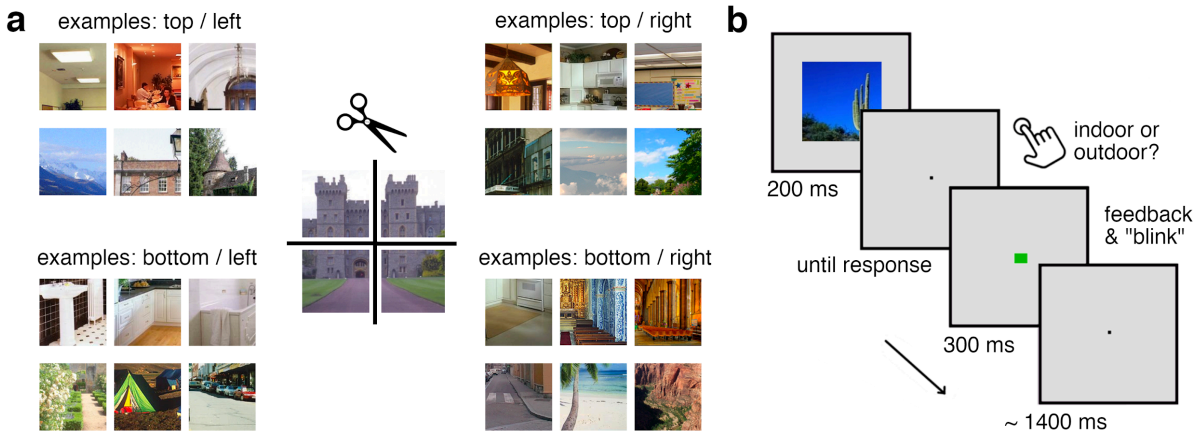

Figure 1. Stimuli and paradigm. a) To mimic the fragmented nature of natural visual inputs, we used a set of 210 widely varying indoor and outdoor scene photographs that each were split into four equally sized fragments (top/left, top/right, bottom/left, bottom/right). The panel shows representative examples from indoor (upper rows) and outdoor (lower rows) scenes. b) During the EEG experiment, participants viewed the individual fragments in the center of the screen while performing an indoor/outdoor categorization task.

Experimental paradigm

During the experiment, participants briefly viewed the individual scene fragments, all presented in the same central location (Figure 1b). Each of the 840 fragments was shown twice during the experiment, yielding 1,680 trials. Trial order was randomized separately for the first and second half of trials, so that every fragment appeared once in the first half of the experiment and once in the second half. On each trial, a single fragment appeared for 200ms and participants were asked to categorize the fragment as either stemming from an indoor scene or an outdoor scene using two keyboard buttons. After every response, the fixation cross turned red or green for 300ms, indicating response correctness. Trials were separated by an inter-trial interval varying randomly between 1,300ms and 1,500ms. Participants performed the categorization task well (93% correct responses, SE=1%; 769ms

144 average response time, SE=36ms), with no differences in accuracy or response time
145 between fragments stemming from the top versus the bottom or from the left versus
146 the right (all $t[19]<1.89$, $p>0.07$). Further, participants were instructed to maintain
147 central fixation throughout the experiment, and to only blink after they had given a
148 response. Stimulus presentation was controlled using the Psychtoolbox (Brainard,
149 1997).
150
151 **EEG recording and preprocessing**
152 EEG signals were recorded using an EASYCAP 64-electrode system and a
153 Brainvision actiCHamp amplifier. Electrodes were arranged in accordance with the
154 10-10 system. EEG data were recorded at 1000Hz sampling rate and filtered online
155 between 0.03Hz and 100Hz. All electrodes were referenced online to the Fz electrode.
156 Offline preprocessing was performed using FieldTrip (Oostenveld et al., 2011). EEG
157 data were epoched from -200ms to 800ms relative to stimulus onset, and baseline-
158 corrected by subtracting the mean pre-stimulus signal. Channels and trials containing
159 excessive noise were removed based on visual inspection. Blinks and eye movement
160 artifacts were removed using independent component analysis and visual inspection
161 of the resulting components. The epoched data were downsampled to 200Hz.
162
163 **Measuring representational similarity**
164 To track the representations of individual fragments across time, we used
165 representational similarity analysis (RSA; Kriegeskorte et al., 2008). First, we created
166 neural representational dissimilarity matrices (RDMs) for each time point in the EEG
167 epochs (5ms resolution), reflecting the pairwise dissimilarity of the fragments' brain

representations. Second, we modeled the organization of the neural RDMs in a regression approach (Proklova et al., 2016, 2019), which allowed us to track when representations are explained by the fragments' vertical and horizontal location within the full scene as well as the scene's category.

To construct neural RDMs, we computed the pairwise dissimilarity of all fragments at each time point using the CoSMoMVPA toolbox (Oosterhof et al., 2016). This analysis was done separately for each participant. For this, we used response patterns across 17 posterior electrodes (Kaiser et al., 2019c) in our EEG montage (O1, O2, Oz, PO3, PO4, PO7, PO8, POz, P1, P2, P3, P4, P5, P6, P7, P8, Pz). For each of the 840 fragments, we computed the response pattern to the fragment by averaging across the two repetitions of the fragment. If after trial rejection during preprocessing only one trial was left for a fragment, we used the response pattern from this one trial. If after preprocessing no trial was left for a fragment, this fragment was excluded from the analysis (i.e., removed from all RDMs of the respective participant). Neural dissimilarity was computed by correlating the response patterns to each individual fragment in a pairwise fashion and subtracting the resulting correlations from 1, yielding an index of neural dissimilarity (0: minimum dissimilarity, 2: maximum dissimilarity). Computing this index for each pairwise comparison of fragments, we obtained an 840-by-840 neural RDM for each time point.

Modelling representational similarity

To quantify how well the neural organization is explained by the fragments' vertical and horizontal location within the full scene and by the original scene's category (indoor vs. outdoor), we modeled the neural RDMs in a general linear model

(GLM) with three predictors: (1) a vertical location RDM, in which each pair of conditions is assigned either a value of 0, if the fragments stem from the same vertical location (e.g., both from the top), or the value 1, if they stem from different vertical locations (e.g., one from the top and one from the bottom), (2) a horizontal location RDM, in which each pair of conditions is assigned either a value of 0, if the fragments stem from the same horizontal location (e.g., both from the left), or the value 1, if they stem from different horizontal locations (e.g., one from the left and one from the right), and (3) a category RDM, in which each pair of conditions is assigned either a value of 0, if the fragments stem from the same scene category (e.g., both from indoor scenes), or the value 1, if they stem from different categories (e.g., one from an indoor scene and one from an outdoor scene).

GLMs were constructed with the neural RDMs as the regression criterion and the vertical and horizontal location RDMs as well as the category RDM as predictors. For these GLMs, the neural RDMs and predictor RDMs were vectorized by selecting all lower off-diagonal elements – the rest of the entries, including the diagonal, were discarded. Values for the neural RDMs were z-scored. Estimating this GLM yielded three beta weights for each time point and participant. We subsequently tested these beta weights across participants against zero, which reveal whether the fragments' vertical location, horizontal location, and their category significantly explained the neural organization at each time point.

We additionally performed two control analyses. In the first control analysis, we assessed if the location-based organization in the fragments' neural representations can be explained by simple visual features. To do so, we used the fragments' similarity in image space to predict their neural organization. We

computed the fragments' image similarity by correlating their pixel values. We then constructed a pixel RDM that contained the fragments' pairwise dissimilarity (1-correlation) in pixel values. To control for image similarity, we ran a GLM in which we predicted neural RDMs as a function of the pixel RDM. In another, second GLM, we then modelled the residuals of the first model using the vertical location, horizontal location, and category predictors (see above). This two-stage approach allowed us to quantify how much vertical and horizontal location information as well as category information remained unaccounted for by the fragments' pixel similarity.

In the second control analysis, we aimed at eliminating visual and conceptual features that are common to either indoor or outdoor scenes (e.g., the top fragments from outdoor scenes often show blue skies). We thus constructed RDMs for horizontal and vertical location information which only contained comparisons across indoor and outdoor scenes. These RDMs were constructed in the same way as explained above, but now all comparisons within the same scene type (e.g., comparisons of different indoor scene fragments) were removed. We then repeated the original GLM analysis (see above) with these restricted RDMs, allowing us to see if the organization according to vertical location persists when only between-category comparisons are considered.

Statistical testing

To test whether GLM beta weights were significantly greater than zero, we used a threshold-free cluster enhancement procedure (Smith and Nichols, 2009) and multiple-comparison correction based on a sign-permutation test (with null distributions created from 10,000 bootstrapping iterations), as implemented in

CoSMoMVPA (Oosterhof et al., 2016). The resulting statistical maps were thresholded at $z>1.64$ (i.e., $p_{corr}<.05$). For all peaks in the time series, we additionally report results of conventional one-sided t-tests against zero. To estimate the robustness of peak latencies we performed a bootstrapping analysis. In this analysis, we created 1000 samples of 20 randomly chosen datasets each (with possible repetitions). For each random sample, we computed the peak latency (i.e., the highest beta estimate in the average time course). We then computed a confidence interval (*ci*) by selecting the central 95% of the distribution across the 1000 random samples. Given the clear two-peak structure in vertical location information, we performed the bootstrapping analysis separately for the early and late peaks, by splitting the data for each random sample along the minimum beta value between 100ms and 200ms.

Data Availability

Data are publicly available on OSF (doi.org/10.17605/OSF.IO/D7P8G).

Results

To model the fragments' cortical representations across time, we ran a GLM analysis with three predictors capturing the fragments' vertical and horizontal locations within the full scene and the full scene's category (Figure 2a). This analysis revealed three key insights. First, the fragments' cortical organization was explained by their vertical location within the scene (Figure 2b), from 70ms to 615ms (peaking at 110ms, peak $t[19]=4.07$, $p<0.001$, $p_{corr}<0.05$, $ci=[85ms, 115ms]$, and at 200ms, peak $t[19]=3.47$, $p=0.001$, $p_{corr}<0.05$, $ci=[190ms, 210ms]$). This suggests that fragmented scene information is sorted by its typical origin within the visual world. Second, the fragments' horizontal location did not significantly predict their neural organization, suggesting that the more rigid real-world location along the vertical axis is more strongly reflected in cortical signals. Third, the fragments' category (i.e., whether a fragment stems from an indoor or an outdoor scene) was also reflected in their neural organization, from 90ms to 800ms (peaking at 330ms, peak $t[19]=3.06$, $p=0.007$, $p_{corr}<0.05$, $ci=[210ms, 635ms]$). This finding supports previous studies showing that scene category can be rapidly decoded from EEG signals (Dima et al., 2018; Kaiser et al., 2019c; Lowe et al., 2019).

Together, these results suggest that fragmented visual information is organized with respect to its typical vertical location in the world. To test how flexible this organization is with respect to visual and conceptual properties of individual scenes, we additionally performed two control analyses.

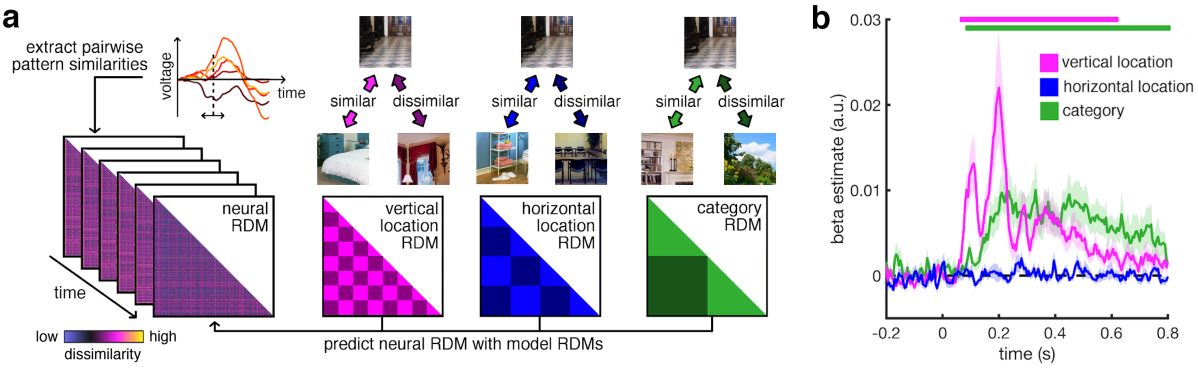

Figure 2. Analysis approach and main result. a) We first extracted neural RDMs from EEG signals in a time-resolved manner. That is, for each time point in an epoch we correlated the response patterns evoked by each one fragment with the response pattern evoked by each other fragment, yielding an 840-by-840 matrix of pairwise neural dissimilarities. The neural RDMs were then modeled as a combination of three predictor RDMs that captured the fragments' dissimilarity in vertical location (e.g. different fragments from the same location were considered similar), horizontal location (e.g. different fragments from the same location were considered similar), and category (e.g. different fragments from the same category were considered similar). Estimating this model for each time point yielded three time courses of beta estimates, indicating how well the neural organization matched each of the predicted organizations. b) The fragments' vertical location (but not their horizontal location) predicted neural organization between 70ms and 615ms, suggesting a sorting of information according to typical real-world locations. Additionally, the fragments' category predicted their neural organization between 90ms and 800ms. Significance markers denote $p_{corr}<0.05$. Shaded margins represent standard errors of the mean.

In the first control analysis, we tested whether simple image features can explain the vertical location organization in the neural data. To quantify such simple visual features, we constructed RDMs from the fragments' pixel values (Figure 3a) and removed these features from the neural data before performing the GLM analysis (see Materials and Methods).

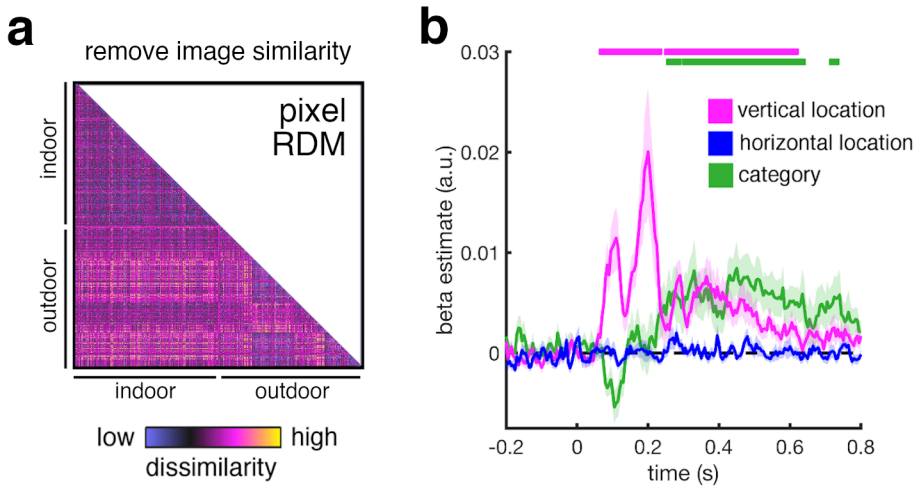

Figure 4. Controlling for image similarity. a) We computed the fragments' low-level visual similarity by computing pairwise dissimilarities (1-correlation) between their pixel values, yielding an 840-by-840 element pixel RDM. We then removed the pixel RDM from the neural organization (see Materials and Methods) before performing the GLM analysis as above, i.e., modelling the fragments' neural organization as a function of their vertical and horizontal locations and their category. d) Removing the fragments' low-level visual similarity did not abolish vertical location information, which remained significant between 70ms and 615ms, suggesting that the sorting of fragments according to their vertical location in the world is flexible with regards to the low-level features. Notably, after removing the pixel RDM, category information emerged only after 260ms, suggesting that the more rapidly emerging vertical location information does not depend on image properties that distinguish the indoor and outdoor scenes. Significance markers denote $p_{corr}<0.05$. Shaded margins represent standard errors of the mean.

After removing the fragments' pixel similarity from the neural RDM, we still found significant vertical location information (Figure 3b), between 70ms and 615ms (peaking at 110ms, peak $t[19]=3.74$, $p<0.001$, $p_{corr}<0.05$, $ci=[85ms, 115ms]$, and at 200ms, peak $t[19]=3.21$, $p=0.002$, $p_{corr}<0.05$, $ci=[190ms, 210ms]$), but no significant horizontal location information. This shows that controlling for simple visual features cannot explain the fragments' neural organization by vertical location. Category

information was still present in the neural data, but now emerged only later, between 260ms and 640ms as well as between 720ms and 730ms (peaking at 450ms, peak $t[19]=3.23$, $p=0.002$, $p_{corr}<0.05$, $ci=[260ms, 720ms]$). This result suggests that during early visual processing vertical location information remains prominent, even if during this time no category information can be observed in the neural data.

In the second control analysis, we more explicitly tested whether the sorting of fragmented information is independent of visual category information by testing if the sorting generalized across indoor and outdoor scenes. In this analysis, we restricted our models to comparisons between indoor and outdoor scenes (i.e., all comparisons within the same scene category were removed from all RDMs). The comparisons between indoor and outdoor scenes share fewer visual and conceptual properties than the comparisons of scenes from the same category (Figure 4a): For example, two fragments from the upper part of outdoor scenes often share both visual properties (e.g., they tend to be blue-colored) and conceptual content (e.g., they tend to contain the same objects, such as clouds of tree tops).

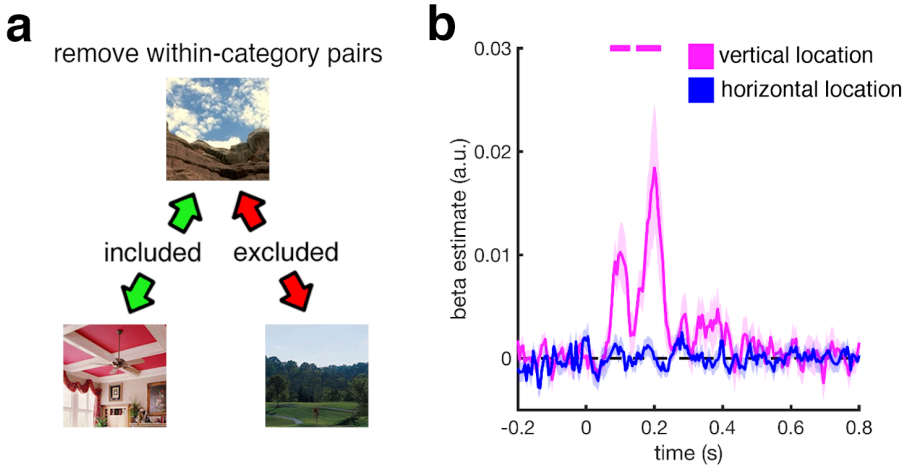

Figure 4. Controlling for similarity within scene category. a) In this analysis, we removed all comparisons between the fragments of the same category from the

neural and predictor RDMs. This allowed us to control for visual and conceptual features shared by fragments stemming from the same location (e.g., fragments from the upper part of outdoor scenes often contain skies and clouds). d) Removing the same-category comparisons did not abolish vertical location information, which remained significant between 80ms and 210ms. This indicates that the sorting of fragments according to their vertical location in the world is flexible with regards to visual and conceptual attributes shared by the scenes of the same category. Significance markers denote $p_{corr}<0.05$. Shaded margins represent standard errors of the mean.

This analysis revealed significant vertical location information (Figure 4b), from 80ms to 120ms (peaking at 100ms, peak $t[19]=3.63$, $p<0.001$, $p_{corr}<0.05$, $ci=$[80ms, 120ms]) and from 155ms to 210ms (peaking at 200ms, peak $t[19]=2.98$, $p=0.004$, $p_{corr}<0.05$, $ci=$[190ms, 215ms]), but no horizontal location information. This suggests that the cortical sorting of information according to the fragments' vertical location occurs similarly for visually and conceptually diverse scenes. Note that – as within-category comparisons were removed – no category information could be computed in this analysis.

Together, our results suggest that fragmented information is sorted according to its typical vertical location in the world, providing a mechanism for the contextualization of incomplete visual information. Even when controlling for visual and conceptual scene attributes, this mechanism can operate rapidly and most strongly determines the cortical organization after 200ms of visual processing.

Discussion

During natural vision the brain is constantly faced with incomplete snapshots of the world from which it needs to infer the structure of the whole scene. Here, we show that in order to meet this challenge, the visual system rapidly contextualizes incoming information according to its typical place in the world: after 200ms of processing, fragmented scene information is sorted according to its real-world location. By using a large stimulus set (comprising 840 unique fragments) we provide compelling evidence that this mechanism supports spatial contextualization across diverse visual environments.

Which features allow the visual system to make such inferences about a fragment's typical position within the environment? Solidifying our previous results (Kaiser et al., 2019c), the strongest organization according to vertical location became apparent at around 200ms after onset. At this time higher-level scene attributes – such as the scene's clutter or openness (Cichy et al., 2017; Harel et al., 2016) – are analyzed, suggesting that the sorting of information according to real-world locations is determined by more complex scene properties, rather than low-level visual features. This is consistent with previous fMRI results which demonstrated a vertical location organization in the occipital place area, but not in early visual cortex (Kaiser et al., 2019c). However, we additionally found a very rapid onset of vertical location information with the first peak shortly after 100ms, which suggests that the visual features extracted during early visual analysis are also diagnostic of a fragment's typical location in the world. Such features could comprise particular distributions of

spatial frequency content or texture information (Dima et al., 2018; Groen et al., 2013, 2017). Alternatively, these early effects could reflect the rapid analysis of scene geometry (Henriksson et al., 2019). Future studies need to isolate the contribution of different visual features to the sorting of visual information by real-world location at different processing times.

Previous research has demonstrated that the representation of individual naturalistic stimuli depends on whether their current position in the visual field matches their typical position in the world (Chan et al., 2010; de Haas et al., 2016; Mannion, 2015; Kaiser & Cichy, 2018; Kaiser et al., 2018). For instance, when face parts (e.g., an eye) or objects (e.g., a lamp) are presented in their typically experienced visual-field position (e.g., the upper visual field), they evoke more efficient cortical representations (de Haas et al., 2016; Kaiser & Cichy, 2018). This suggests that across diverse visual contents cortical representations of a stimulus are entwined with preferences for its typical location (Kaiser & Haselhuhn, 2017; Kaiser et al., 2019a). Here we show that the pairing of visual representations and location information is apparent even when objects do not appear in their expected locations: although in the current study all fragments were presented in the same central location, their representations were still organized by their typical location. This shows that even in the absence of location information the brain can use the characteristic spatial distribution of visual contents to organize their representation in an efficient way. A related effect of real-world structure on individual object representations was previously reported in face processing, where representations of individual face fragments are grouped according to their position within a face (Henriksson et al., 2015). Together, these results suggest that information across different types of

fragmented visual contents can be contextualized on the basis of real-world structure.

How does this contextualization mechanism aid perception under naturalistic conditions? The mechanism may be particularly beneficial across a variety of situations where visual inputs are incomplete. Such situations include partially occluded objects, fast-changing and dynamic environments, and fragmented information arising from eye movements across a scene. In each of these situations, matching the input with its typical position in the context of the current environment can facilitate the understanding of the incomplete information available at every point in time. Future studies need to connect the rapid sorting process described here and behavioral benefits in the aforementioned situations.

Acknowledgements

D.K. and R.M.C. are supported by Deutsche Forschungsgemeinschaft (DFG) grants (KA4683/2-1, CI241/1-1, CI241/3-1). R.M.C. is supported by a European Research Council Starting Grant (ERC-2018-StG 803370). The authors declare no conflict of interest.

Author Contributions

D. K. and R.M.C. designed research, D.K. and G.I. acquired data, D.K. and G.I. analyzed data, D.K., G.I., and R.M.C. interpreted results, D.K. prepared figures, D.K. drafted manuscript, D.K., G.I., and R.M.C. edited and revised manuscript. All authors approved the final version of the manuscript.

441

442 **References**

443

444 Abassi, E., & Papeo, L. (2019). The representation of two-body shapes in the human
445 visual cortex. *Journal of Neuroscience*, doi.org/10.1523/JNEUROSCI.1378-
446 19.2019

447 Baldassano, C., Beck, D. M., & Fei-Fei, L. (2017). Human-object interactions are more
448 than the sum of their parts. *Cerebral Cortex, 27*, 2276-2288.

449 Bar, M. (2004). Visual objects in context. *Nature Reviews Neuroscience, 5,* 617-629.

450 Bilalic, M., Lindig, T., & Turella, L. (2019). Parsing rooms: the role of the PPA and RSC
451 in perceiving object relations and spatial layout. *Brain Structure and Function,*
452 *224*, 2505-2524.

453 Brainard, D. H. (1997). The psychophysics toolbox. *Spatial Vision, 10*, 433-436.

454 Chan, A. W., Kravitz, D. J., Truong, S., Arizpe, J., & Baker, C.I. (2010). Cortical
455 representations of bodies and faces are strongest in commonly experienced
456 configurations. *Nature Neuroscience, 13,* 417-418.

457 Cichy, R. M., Khosla, A., Pantazis, D., & Oliva, A. (2017). Dynamics of scene
458 representations in the human brain revealed by magnetoencephalography and
459 deep neural networks. *NeuroImage, 153*, 346-358.

460 de Haas, B., Schwarzkopf, D. S., Alvarez, I., Lawson, R. P., Henriksson, L.,
461 Kriegeskorte, N., & Rees, G. (2016). Perception and processing of faces in the
462 human brain is tuned to typical facial feature locations. *Journal of*
463 *Neuroscience, 36,* 9289-9302.

464 Dima, D. C., Perry, G., & Singh, K. D. (2018). Spatial frequency supports the
465 emergence of categorical representations in visual cortex during natural scene
466 perception. *Neuroimage, 179*, 102-116.
467 Geisler, W. S. (2008). Visual perception and the statistical properties of natural
468 scenes. *Annual Review of Psychology, 59*, 167-192.
469 Groen, I. I., Ghebreab, S., Prins, H., Lamme, V. A., & Scholte, H.S. (2013). From image
470 statistics to scene gist: evoked neural activity reveals transition from low-level
471 natural image structure to scene category. *Journal of Neuroscience, 33*, 18814-
472 18824.
473 Groen, I. I., Silson, E. H., & Baker, C. I. (2017). Contributions of low- and high-level
474 properties to neural processing of visual scenes in the human brain.
475 *Philosophical Transactions of the Royal Society B – Biological Sciences, 372*.
476 Gronau, N., Neta, M., & Bar, M. (2008). Integrated contextual representation for
477 objects' identities and their locations. *Journal of Cognitive Neuroscience, 20*,
478 371-388
479 Harel, A., Groen, I. I. A., Kravitz, D. J., Deouell, L. Y., & Baker, C. I. (2016). The
480 temporal dynamics of scene processing: A multifaceted EEG investigation.
481 *eNeuro, 3*, ENEURO.0139-16.2016.
482 Henriksson, L., Mur, M., & Kriegeskorte, N. (2015). Faciotopy – A face-feature map
483 with face-like topography in the human occipital face area. *Cortex, 72,* 156-
484 167.
485 Henriksson, L., Mur, M., & Kriegeskorte, N. (2019). Rapid invariant encoding of scene
486 layout in human OPA. *Neuron, 103*, 161-171.

Kaiser, D., & Cichy, R. M. (2018). Typical visual-field locations enhance processing in object-selective channels of human occipital cortex. *Journal of Neurophysiology*, *120*, 848-853.

Kaiser, D., Häberle, G., & Cichy, R. M. (2019b) Cortical sensitivity to natural scene structure. *Human Brain Mapping,* doi.org/10.1002/hbm.24875

Kaiser, D., & Haselhuhn, T. (2017). Facing a regular world: How spatial object structure shapes visual processing. *Journal of Neuroscience, 37,* 1965-1967.

Kaiser, D., Moeskops, M. M., & Cichy, R. M. (2018). Typical retinotopic locations impact the time course of object coding. *NeuroImage, 176*, 372-379.

Kaiser, D., & Peelen, M. V. (2018). Transformation from independent to integrative coding of multi-object arrangements in human visual cortex. *NeuroImage 169*, 334-341.

Kaiser, D., Quek, G. L., Cichy, R. M., & Peelen, M. V. (2019a). Object vision in a structured world. *Trends in Cognitive Sciences, 23*, 672-685.

Kaiser, D., Stein, T., & Peelen, M. V. (2014). Object grouping based on real-world regularities facilitates perception by reducing competitive interactions in visual cortex. *Proceedings of the National Academy of Sciences USA, 111*, 11217-11222.

Kaiser, D., Turini, J., & Cichy, R. M. (2019c). A neural mechanism for contextualizing fragmented inputs during naturalistic vision. *eLife, 8*, e48182.

Kim, J. G., & Biederman, I. (2011). Where do objects become scenes? *Cerebral Cortex, 21*, 1738-1746.

Kim, J. G., Biederman, I., & Juan, C. H. (2011). The benefit of object interactions arises in the lateral occipital cortex independently of attentional modulation from the

intraparietal sulcus: a transcranial magnetic stimulation study. *Journal of Neuroscience, 31*, 8320-8324.

Konkle, T., Brady, T. F., Alvarez, G. A., & Oliva, A. (2010). Scene memory is more detailed than you think: the role of categories in visual long-term memory. *Psychological Science, 21*, 1551-1556.

Kriegeskorte, N., Mur, M., & Bandettini, P. (2008). Representational similarity analysis – connecting the branches of systems neuroscience. *Frontiers in Systems Neuroscience, 2,* 4.

Lowe, M. X., Rajsic, J., Ferber, S., & Walther, D. B. (2018). Discriminating scene categories from brain activity within 100 milliseconds. *Cortex, 106*, 275-287.

Mandler, J. M. (1984). Stories, scripts and scenes: aspects of schema theory. L. Erlbaum.

Mandler, J. M., & Parker, R. E. (1976). Memory for descriptive and spatial information in complex pictures. *Journal of Experimental Psychology: Human Learning, Memory, & Cognition, 2,* 38-48.

Mannion, D. J. (2015). Sensitivity to the visual field origin of natural image patches in human low-level visual cortex. *PeerJ, 3*, e1038.

Minsky, M. (1975). A framework for representing knowledge. In: The psychology of computer vision. Winston, P. (ed), McGraw-Hill.

Oliva, A., & Torralba, A. (2003). Statistics of natural image categories. *Network, 14,* 391-412.

Oliva, A., & Torralba, A. (2007). The role of context in object recognition. *Trends in Cognitive Sciences, 11*, 520-527.

534 Oostenveld, R., Fries, P., Maris, E., & Schoffelen, J. M. (2011). FieldTrip: Open source
535 software for advanced analysis of MEG, EEG, and invasive
536 electrophysiological data. *Computational Intelligence and Neuroscience, 2011,*
537 156869.
538 Oosterhof, N. N., Connolly, A. C., & Haxby, J V. (2016). CoSMoMVPA: Multi-modal
539 multivariate pattern analysis of neuroimaging data in Matlab/GNU Octave.
540 *Frontiers in Neuroinformatics, 10,* 20.
541 Proklova, D., Kaiser, D., & Peelen, M. V. (2016). Disentangling representations of
542 object shape and object category in human visual cortex: the animate-
543 inanimate distinction. *Journal of Cognitive Neuroscience, 28*, 680-692.
544 Proklova, D., Kaiser, D., & Peelen, M. V. (2019). MEG sensor patterns reflect
545 perceptual but not categorical similarity of animate and inanimate objects.
546 *Neuroimage, 192*, 167-177.
547 Purves, D., Wojtach, W. T., & Lotto, R. B. (2011). Understanding vision in wholly
548 empirical terms. *Proceedings of the National Academy of Sciences USA, 108*,
549 15588-15595.
550 Roberts, K. L., & Humphreys, G. W. (2010). Action relationships concatenate
551 representations of separate objects in the ventral visual cortex. *NeuroImage*
552 *52*, 1541-1548.
553 Rumelhart, D. E. (1980). Schemata: the building blocks of cognition. In: Theoretical
554 issues in reading comprehension. Spiro R. J., et al. (eds.), L. Erlbaum.
555 Smith, S. M., & Nichols, T. E. (2009). Threshold-free cluster enhancement: addressing
556 problems of smoothing, threshold dependence and localisation in cluster
557 inference. *NeuroImage, 44,* 83-98.

Torralba, A., Oliva, A, Castelhano, M. S., & Henderson, J. M. (2006). Contextual guidance of eye movements and attention in real-world scenes: the role of global features in objects search. *Psychological Review, 113,* 766-786.

Võ, M. L.-H., Boettcher, S. E. P., & Draschkow, D. (2019). Reading scenes: How scene grammar guides attention and aids perception in real-world environments. *Current Opinion in Psychology, 29*, 205-210.

Wolfe, J. M., Võ, M. L.-H., Evans, K. K., & Greene, M. R. (2011). Visual search in scenes involves selective and nonselective pathways. *Trends in Cognitive Sciences, 15,* 77-84.